SCIENTIFIC REPORTS

OPEN

SUBJECT AREAS:
EXPERIMENTAL MODELS OF DISEASE
ACUTE INFLAMMATION

Received
6 November 2013

Accepted
4 April 2014

Published
24 April 2014

Correspondence and requests for materials should be addressed to X.D.Y. (yang.xiangdong@zs-hospital.sh.cn) or J.B.G. (ge.junbo@zs-hospital.sh.cn)

* These authors contributed equally to this work.

Hydrogen Sulfide Attenuates the Recruitment of CD11b$^+$Gr-1$^+$ Myeloid Cells and Regulates Bax/Bcl-2 Signaling in Myocardial Ischemia Injury

Youen Zhang[1]*, Hua Li[1,2]*, Gang Zhao[1], Aijun Sun[1,3], Nobel C. Zong[2,4], Zhaofeng Li[1], Hongming Zhu[2], Yunzeng Zou[1,3], Xiangdong Yang[1] & Junbo Ge[1,3]

[1]Shanghai Institute of Cardiovascular Diseases, Zhongshan Hospital, Fudan University, Shanghai, 200032, China, [2]Departments of Physiology and Medicine/CVRL, UCLA School of Medicine, Los Angeles, California, 90095, USA, [3]Institutes of Biomedical Sciences, Fudan University, Shanghai, 200032, China, [4]NHLBI Proteomics Center at UCLA/NHLBI Proteomics Program, UCLA School of Medicine, Los Angeles, California, 90095, USA.

Hydrogen sulfide, an endogenous signaling molecule, plays an important role in the physiology and pathophysiology of the cardiovascular system. Using a mouse model of myocardial infarction, we investigated the anti-inflammatory and anti-apoptotic effects of the H_2S donor sodium hydrosulfide (NaHS). The results demonstrated that the administration of NaHS improved survival, preserved left ventricular function, limited infarct size, and improved H_2S levels in cardiac tissue to attenuate the recruitment of CD11b$^+$Gr-1$^+$ myeloid cells and to regulate the Bax/Bcl-2 pathway. Furthermore, the cardioprotective effects of NaHS were enhanced by inhibiting the migration of CD11b$^+$Gr-1$^+$ myeloid cells from the spleen into the blood and by attenuating post-infarction inflammation. These observations suggest that the novel mechanism underlying the cardioprotective function of H_2S is secondary to a combination of attenuation the recruitment of CD11b$^+$Gr-1$^+$ myeloid cells and regulation of the Bax/Bcl-2 apoptotic signaling.

Hydrogen sulfide (H_2S) has long been recognized as a toxic, colorless gas with a characteristic rotten-egg odor that is found in various natural and industrial products. However, recent accumulated data have demonstrated that H_2S exerts a host of biological effects on various targets, ranging from cytotoxic to cytoprotective effects[1,2]. Among these effects is a steadily growing list of physiological functions in mammals that affect blood pressure, oxidative stress, inflammation, and insulin secretion. Endogenous H_2S is produced enzymatically by the cysteine metabolic enzymes cystathionine β-synthase (CBS), cystathionine γ-lyase (CSE), and 3-mercaptopyruvate sulfurtransferase[1]. The ability of H_2S to function as a signaling molecule at low micromolar levels in mammalian systems parallels the action of another established gasotransmitter, nitric oxide (NO)[3]. In particular, H_2S exhibits almost all of the beneficial cardiovascular effects of NO without the deleterious production of reactive oxygen species (ROS), acting instead as a scavenger of ROS. Other studies have indicated that the administration of the H_2S donor sodium hydrosulfide (NaHS) could attenuate ischemia/reperfusion (I/R) injury in the heart, liver, and kidneys by opening K_{ATP} channels[4,5]. Transplantation of exogenous H_2S-pretreated mesenchymal stem cells (MSCs) reduced infarct size and increased left ventricular function in a rat myocardial infarction (MI) model[6]. These studies suggest that NaHS has anti-inflammatory effects and modulates innate immune cells[7,8].

Undifferentiated monocytes in the red pulp of the spleen are activated and migrate to areas of tissue that have suffered ischemic myocardial injury[9]. CD11b$^+$Gr-1$^+$ myeloid cells are among the immunosuppressive cells in the spleen and bone marrow[10]. In conditions with multiple inflammatory stimuli, such as DSS-induced colitis and TPA-induced skin inflammation, the number of CD11b$^+$Gr-1$^+$ myeloid cells is markedly increased in the circulation, as these cells are released from the spleen and bone marrow to perform related immune functions[11].

In the present study, we used a murine MI model to test the hypothesis that the administration of NaHS pre- and post-coronary artery occlusion could protect the heart from myocardial injury and improve survival; we further explored the mechanism of NaHS-mediated cardioprotection, specifically the regulation of

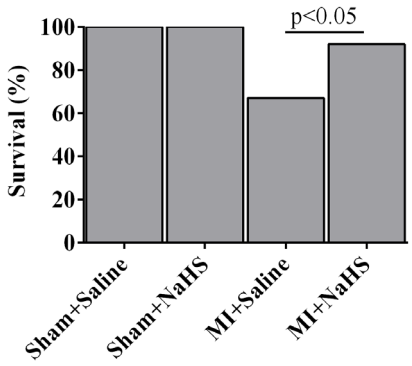

Figure 1 | Survival of the mice in the different groups at 24 hrs post-MI. Note that the NaHS-treated MI mice exhibited a significant increase in survival compared with the MI + Saline animals.

$CD11b^+Gr\text{-}1^+$ myeloid cells and Bax/Bcl-2 apoptotic signaling. The findings provided a novel insight into the cardioprotective role of H_2S in the pathophysiology of MI and the post-MI immune response, and they improved our understanding of clinical therapies for the cardiovascular system.

Results

NaHS improves survival. The survival was 100% in the sham-operated mice, while 29 of 32 (91%) mice in the MI + NaHS group survived, compared with 21 of 32 (66%) in the MI + Saline group (Fig. 1). The causes of death in each group are summarized in Table 1. The most frequent cause of post-MI death in both MI groups was ventricular rupture (45% in MI + Saline versus 33% in MI + NaHS), which occurred within 24 hrs post-MI.

NaHS preserves left ventricular function after MI. Acute MI in mice causes a myriad of hemodynamic stresses, which trigger left ventricular remodeling and eventually lead to functional decompensation and heart failure. To evaluate the effects of exogenous H_2S on the left ventricular function of the mice with MI, the surviving animals were evaluated with two-dimensional, high-resolution echocardiography (Fig. 2A). None of the groups presented significant LV dilatation at 24 hrs after infarction (Fig. 2B). However, the mice that were treated with NaHS displayed a significantly decreased LV end-systolic diameter (Fig. 2C) and a more preserved ejection fraction (Fig. 2D), compared with the MI + Saline mice.

NaHS limits the myocardial infarct size. Representative photomicrographs of mid-ventricular cross-sections of TTC-stained hearts are shown in Fig. 3A. Consistent with the improvement in cardiac function (Fig. 2), the photomicrographs show a smaller infarct size (% of left ventricular) at 24 hrs after infarction (Fig. 3B) in the NaHS-treated group.

NaHS improves H_2S levels in post-MI cardiac tissue. Next, we determined whether an exogenous H_2S donor could affect the H_2S levels in cardiac tissue that was under ischemic stress. Fig. 4 illustrates a significant decrease in H_2S in the injured myocardium, compared with the sham group ($P < 0.01$). However, treatment with NaHS mitigated the decrease in H_2S that was seen in the MI + Saline group ($P < 0.01$), showing no difference compared with the sham group ($P > 0.05$).

Cardiac tissue H_2S inhibits the post-MI recruitment of $CD11b^+Gr\text{-}1^+$ myeloid cells. To elucidate the effects of H2S on immune activation and infiltration into the infarcted heart, we quantified the immune cells in the heart with the myeloid cell surface markers CD11b and Gr-1. FACS analysis showed that $CD11b^+Gr\text{-}1^+$ myeloid cells were significantly increased in the heart after infarction, compared with the sham group ($P < 0.01$). However, NaHS treatment significantly reduced the recruitment of $CD11b^+Gr\text{-}1^+$ myeloid cells seen in the MI + Saline group (Fig. 5B).

Cardiac tissue H_2S reduces post-MI cardiomyocyte apoptosis *in vivo*. Immunoblots revealed that the expression of Bax was significantly reduced, while Bcl-2 expression was increased in the hearts following 24 hrs of treatment with NaHS, compared to the expression levels in the MI + Saline group (Figs. 6B and 6C). Consequently, the ratio of Bcl-2 to Bax was increased in the MI + NaHS mice, compared with the MI + Saline mice (Fig. 6D). This result was confirmed using another apoptotic marker, activated caspase 3 (Fig. 6E). Consistent with the known roles of Bax and Bcl-2 in apoptosis, the percentage of TUNEL-positive (apoptotic) cardiomyocytes in the infarcted heart was lower in animals treated with NaHS than in the MI + Saline mice (Figs. 6F and 6G).

NaHS inhibits the migration of $CD11b^+Gr\text{-}1^+$ myeloid cells. To gain further insight into the relationship between H_2S and $CD11b^+Gr\text{-}1^+$ myeloid cells in this MI model, we determined the numbers of $CD11b^+Gr\text{-}1^+$ myeloid cells in the peripheral blood and the spleen. We found that the number of myeloid cells significantly increased in the blood after infarction (Fig. 7B). Administration of H_2S, however, reduced the number of circulating $CD11b^+Gr\text{-}1^+$ myeloid cells, compared with the number seen in the MI + Saline group. Additionally, NaHS resulted in more $CD11b^+Gr\text{-}1^+$ myeloid cells in the reservoir spleen of MI + NaHS, compared with MI + Saline (Fig. 7D).

NaHS reduces post-MI inflammation. To investigate the effects of NaHS on the inflammatory response, the serum levels of TNFα and IL-1β were measured at 24 hrs post-MI. ELISA analysis revealed significant increases in both TNFα and IL-1β in the MI + Saline group, compared with the sham group (Figs. 8A and 8B). However, NaHS treatment mitigated the increases in TNFα and IL-1β levels that were seen in the MI + Saline group (41.2 ± 4.1 versus 53.0 ± 4.7 pg/mL, 162.0 ± 19.1 versus 267.2 ± 25.2 pg/mL, respectively).

Discussion

Left ventricular remodeling after acute MI causes heart failure, which is an epidemic with high mortality and an increasing prevalence. Despite advances in medical and interventional therapy for MI that have dramatically improved survival rates, many surviving patients continue to develop heart failure[12]. Emerging evidence from experimental models of myocardial ischemia has suggested that defects in the timely suppression, resolution, and containment of post-infarction inflammatory responses result in adverse remodeling of the

Table 1 | Causes of death of mice that suffered from an MI

Conditions	Sham + Saline	Sham + NaHS	MI + Saline	MI + NaHS
Ventricular Rupture	0	0	5	1
Acute Heart Failure	0	0	2	0
Bleeding	0	0	1	1
Unknown Reasons	0	0	3	1
Total Death	0	0	11	3

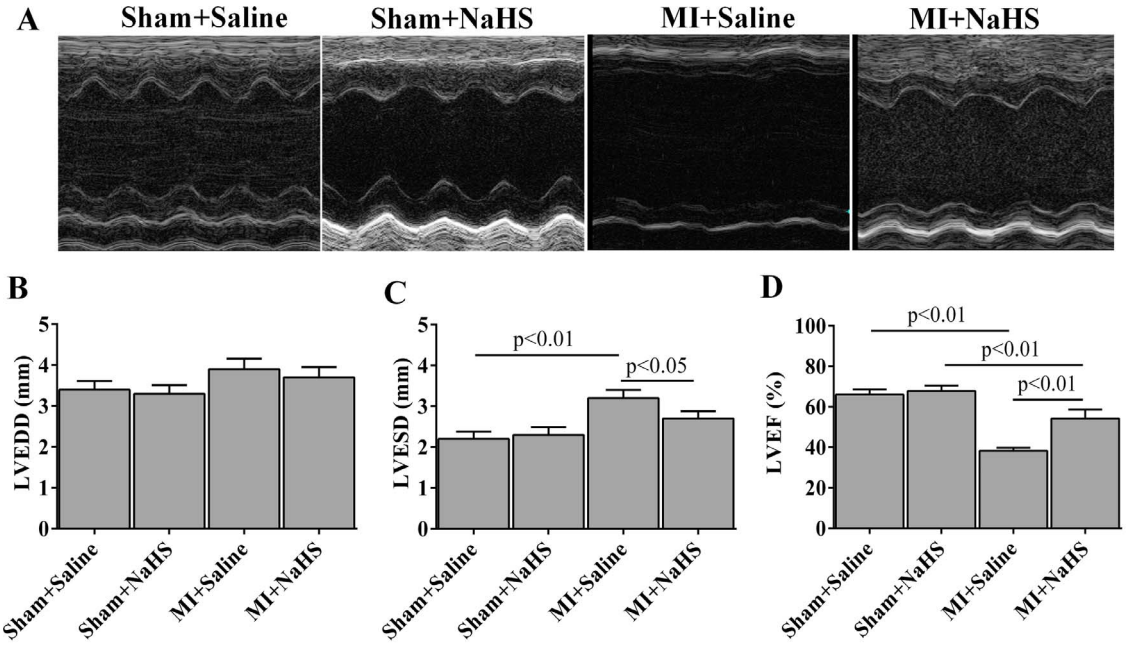

Figure 2 | Cardiac function measured by echocardiography at 24 hrs post-surgery. (A) Representative M-mode images from individual groups. (B–D) Left ventricular end-diastolic diameter (LVEDD), end-systolic diameter (LVESD), and ejection fraction (LVEF) were calculated for the different treatment groups (n = 8).

infarcted heart[13,14]. A recent study in a mouse model reported substantial changes in the immune response dynamics after permanent (MI) or transient (IR) ligation of the left anterior descending artery[15,16]. Inflammation signals recruit neutrophils to the infarcted zone within 24 hrs, and the recruitment of monocytes/macrophages occurs shortly thereafter. In the infarcted myocardium, several innate immune pathways participate in the early steps of the inflammatory response following infarction, including pathways that involve the membrane-bound Toll-like receptors (TLRs), the high-mobility group box 1, and the complement system. Understanding the "STOP" signals involved in suppression of inflammation following infarction might be the key to preventing adverse remodeling and progression to heart failure[13,17].

As a gasotransmitter, H_2S is able to diffuse freely across cell membranes in a receptor-independent manner and to activate various cellular signals that modulate metabolism, cardiac function, and cell survival. These distinct abilities make H_2S an attractive pharmacological agent for the treatment of cardiovascular disease[18]. Several experimental approaches have shown that increased levels of H_2S exert cyto- and cardioprotective effects in the injured myocardium. The results can be achieved both by increasing the endogenous amount of H_2S and by adding exogenous H_2S (the most commonly used H_2S donors are NaHS and Na_2S)[19,20]. Specifically, cardiac-restricted overexpression of CSE resulted in increased H_2S bioavailability and elicited a cardioprotective response to ischemic heart failure and acute myocardial I/R injury[21]. In contrast, decreased production of this molecule has been associated with increased myocardial damage[22,23]. In this study, our results indicated that NaHS could attenuate myocardial ischemic injury, preserve left ventricular function, and enhance survival following infarction.

Because $CD11b^+Gr\text{-}1^+$ myeloid cells are among the primary immunosuppressive factors in cancer and other pathological conditions, several different therapeutic strategies that target these cells are currently being explored[24,25]. Although the studies described were undertaken in tumor-bearing hosts, it is likely that similar strategies aimed at inhibiting or eliminating $CD11b^+Gr\text{-}1^+$ myeloid cells will be therapeutically useful in other pathological conditions. In previous studies, the balance of histamine within the tumor microenvironment was found to be a critical factor, and $CD11b^+Gr\text{-}1^+$ myeloid cells represented an important therapeutic target for the control of cancer growth[11]. An increasing amount of evidence has indicated that $CD11b^+Gr\text{-}1^+$ myeloid cells play an important role in physiological and pathological conditions. Related research reported that myocardial I/R induced a surge in $CD11b^+Gr\text{-}1^+$ neutrophil

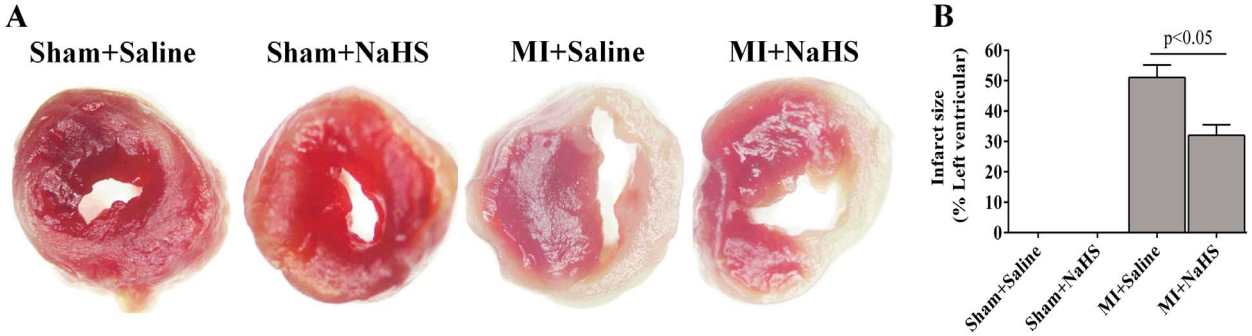

Figure 3 | The infarct size measured at 24 hrs post-MI in the different groups. (A) Representative mid-myocardial cross-sections of TTC-stained hearts. White area, infarcted tissue; red, viable myocardium. (B) The infarcted size, expressed as a percentage of the left ventricle (n = 5–6).

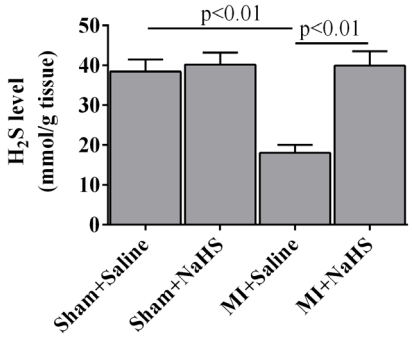

Figure 4 | NaHS therapy improves the level of H_2S. Note that NaHS caused an increase in level of cardiac tissue H_2S after infarction (n = 4–5).

recruitment to the myocardium, and treatment with anti-IL-17A mAb reduced this effect[26]. In the current study, we found that NaHS could protect against ischemic myocardial injury by reducing the recruitment of $CD11b^+$ $Gr\text{-}1^+$ myeloid cells to the myocardium, inhibiting the migration of these cells from the splenic reservoir, and decreasing the induced expression of TNFα and IL-1β in the serum following ischemic injury.

Both permanent coronary occlusion and I/R caused large amounts of myocytes and nonmyocytes to undergo apoptosis within the ischemic zone[27,28]. This excessive or inappropriate apoptosis contributed to pathological changes in the heart. The cardioprotective effects of H_2S in the setting of myocardial I/R in mice were reportedly mediated in large part by a combination of antioxidant and anti-apoptotic signaling[29]. In addition to its well-known immunosuppressant properties, cyclosporine is a potent inhibitor of mitochondrial permeability transition pore opening, which is an important step in programmed cell death. In a small pilot trial of 58 patients with acute ST-elevation myocardial infarction, an intravenous bolus of cyclosporine immediately before percutaneous coronary intervention was associated with a smaller infarct than that seen with placebo[30]. Neutrophil recruitment played a major role in myocardial damage after ischemia injury[31]. In the present study, H_2S inhibited the recruitment of $CD11b^+Gr\text{-}1^+$ myeloid cells to the myocardium and attenuated the post-MI inflammatory response. Our results also revealed that H_2S reduced the expression level of the pro-apoptotic protein Bax and induced the expression of the anti-apoptotic protein Bcl-2, therefore causing an increase in the ratio of Bcl-2/Bax, as confirmed by the change in caspase 3 activity, and resulting in fewer TUNEL-positive (apoptotic) cardiomyocytes.

In fact, moderate use of H_2S balneotherapy (treatment by bathing) has been shown to raise tolerance to exercise and reduce the daily need for short-acting nitrates in patients with coronary artery disease[32]. Moreover, recent clinical data have suggested that total plasma sulfide levels are negatively correlated with the severity of congestive heart failure and that low total plasma sulfide levels predict higher mortality[33]. The current study shows that NaHS, when administered to mice in two separate doses, significantly enhances the generation of H_2S in cardiac tissue, reduces inflammation, attenuates left ventricular dysfunction 24 hrs after ischemic myocardial injury, and hence improves survival.

In conclusion, we demonstrated that NaHS has potent anti-inflammatory and anti-apoptotic effects in heart subjected to acute MI *in vivo*. These cardioprotective functions of NaHS are secondary to a combination of anti-inflammatory and anti-apoptotic effects. Moreover, the anti-inflammatory function may be in part due to the limitation of the recruitment of $CD11b^+Gr\text{-}1^+$ myeloid cells. Additional insight into the control of $CD11b^+Gr\text{-}1^+$ myeloid cells by H_2S treatment will not only illuminate the fundamental molecular principles of $CD11b^+Gr\text{-}1^+$ myeloid cells regulation but will facilitate the therapeutic value in the clinical setting of myocardial ischemia injury.

Methods

Animals. C57BL/6J mice (20–25 g, male, 8–10 weeks; Slac Laboratory, Shanghai, China) were housed under standard conditions in an animal room with a 12/12 h day/night cycle with free access to water and food. This study was performed in strict accordance with the recommendations from the Guide for Animal Management Rules from the Ministry of Health of the People's Republic of China. The protocol was approved by the Committee on the Ethics of Animal Experiments of Fudan University. All of the surgeries were performed under anesthesia, and the utmost effort was exerted to prevent suffering and minimize the numbers of mice required for each experiment.

H_2S donor. H_2S was administered in the form of NaHS, which was obtained from Sigma-Aldrich. NaHS was diluted in normal (0.9%) saline to the desired concentration immediately before administration.

Myocardial infarction protocol. Surgery to induce myocardial infarction was performed in the mice as described previously[34]. In brief, the mice were anesthetized by inhalation of isoflurane, were intubated with a 22-G intravenous catheter, and then were fully anesthetized with 1.0–2.0% isoflurane gas while being mechanically ventilated on a positive pressure ventilator. Left thoracotomy was performed at the fourth intercostal space, and the pericardium was stripped to expose the heart. The left descending coronary artery was identified and occluded with an 8–0 silk ligature that was placed around it. The success of the ligation was confirmed when the anterior wall of the left ventricle turned pale. The chest cavity was closed, and the animal was placed in a cage on a heating pad. Sham-operated mice underwent the same surgical procedures except that the suture placed under the left anterior descending artery was not tied.

Experimental groups. Four groups were used: 1) Sham + Saline: each mouse received 1 mg/kg normal (0.9%) saline (i.p.) 5 minutes before surgery and 60 minutes after sham operation; 2) Sham + NaHS: mice received 1 mg/kg NaHS (i.p.) 5 minutes before surgery and 60 minutes after sham operation; 3) MI + Saline: 1 mg/kg normal (0.9%) saline was administered as in group 1; and 4) MI + NaHS: 1 mg/kg NaHS was administered as in group 2.

Survival. The survival rate was measured based on the animals that survived the experimental protocol starting from recovery after surgery until 24 hrs after

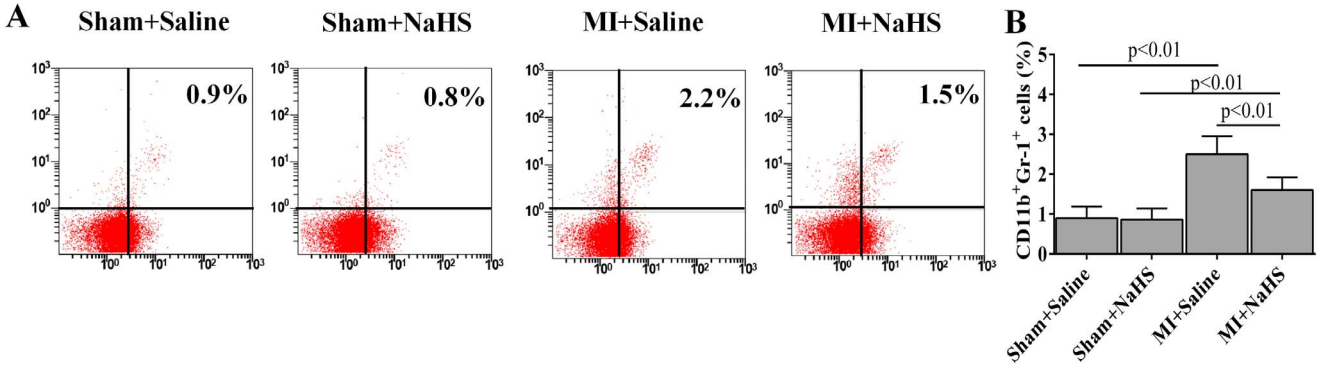

Figure 5 | NaHS inhibits the recruitment of $CD11b^+Gr\text{-}1^+$ myeloid cells. (A) Representative flow cytometry dot plots of the $CD11b^+Gr\text{-}1^+$ myeloid cells that infiltrated into the myocardium 24 hrs post-MI. (B) The percentage of $CD11b^+Gr\text{-}1^+$ cells that infiltrated into the myocardium (n = 6).

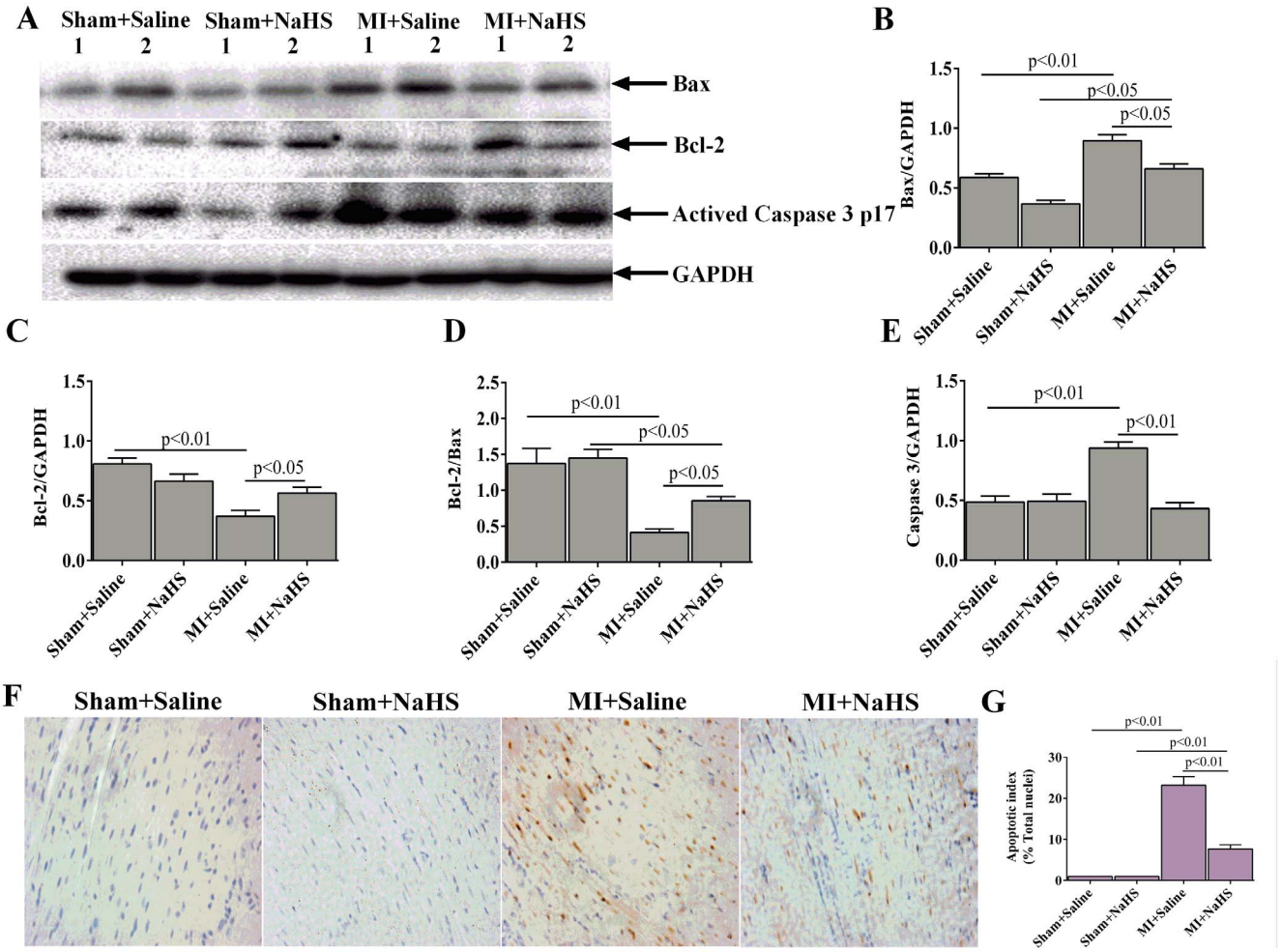

Figure 6 | **H_2S reduces cardiomyocyte apoptosis *in vivo*.** (A) Representative immunoblots showing the expression of Bax, Bcl-2, and activated caspase 3 p17 in the heart. Bax (B) and Bcl-2 (C) expression normalized to GAPDH (n = 6). (D) Densitometric analysis of the ratio of Bcl-2 to Bax. (E) Activated caspase 3 p17 expression normalized to GAPDH (n = 6). (F) Representative photomicrographs of heart sections showing TUNEL-positive (apoptotic) myocardiocytes (200×). (G) Quantification of the apoptotic cells (% total nuclei, n = 6).

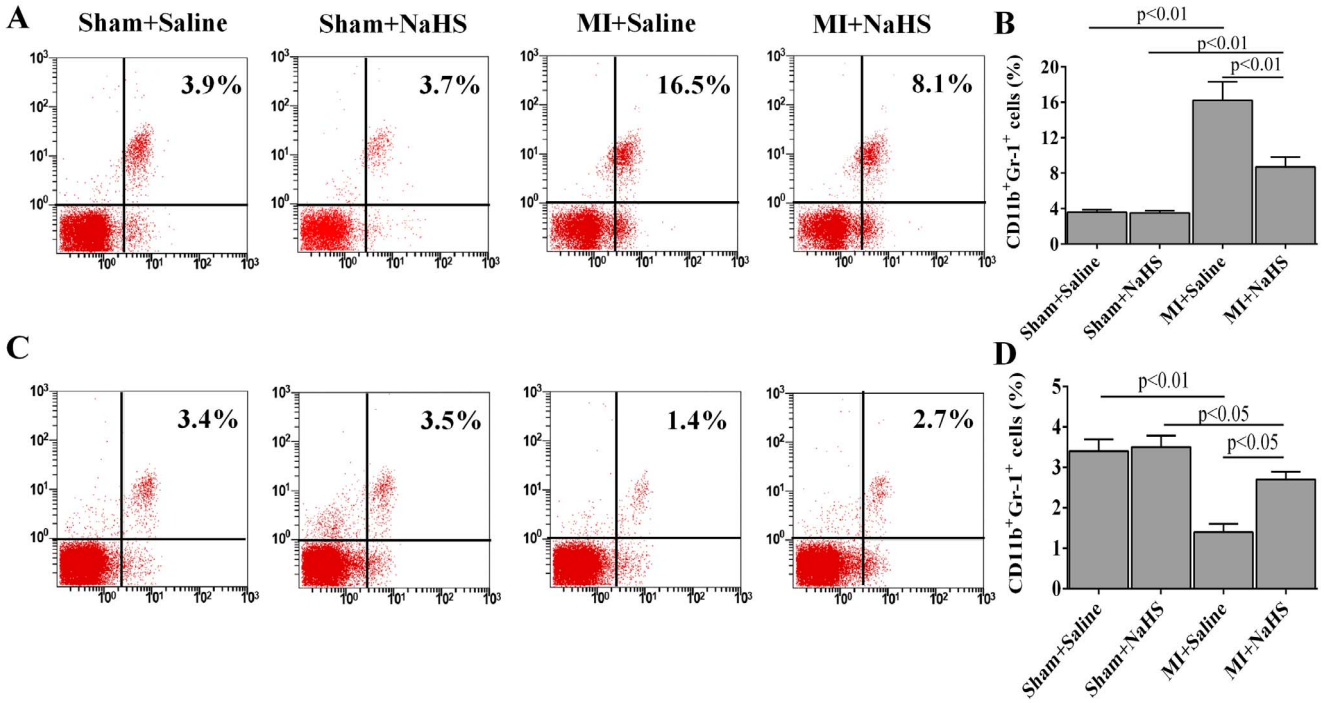

Figure 7 | **NaHS inhibits the migration of $CD11b^+Gr\text{-}1^+$ myeloid cells.** Representative flow cytometry dot plots of $CD11b^+Gr\text{-}1^+$ myeloid cells in the blood (A) and the spleen (C) 24 hrs post-MI. The percentage of $CD11b^+Gr\text{-}1^+$ cells in the blood (B, n = 6) and the spleen (D, n = 6).

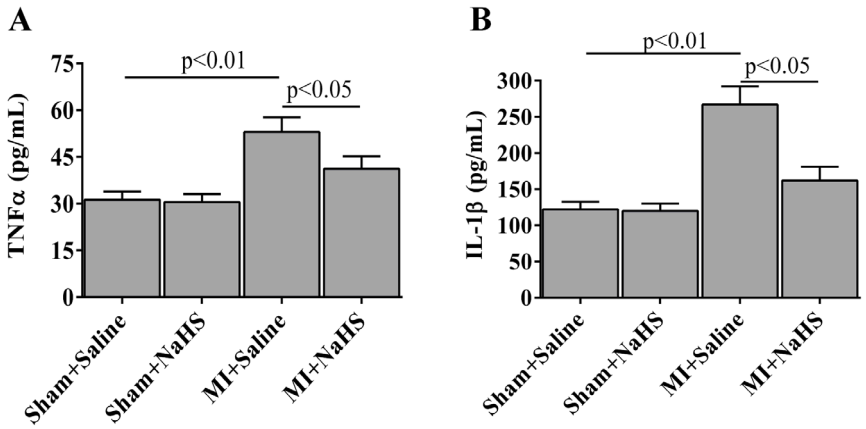

Figure 8 | NaHS inhibits the extent of inflammation. The TNFα (A) and IL-1β (B) levels were significantly decreased in mice treated with an NaHS donor 24 hrs after infarction (n = 6).

infarction. An autopsy was performed on each animal found dead or sacrificed after 24 hrs.

Echocardiography. Transthoracic echocardiography was performed using the Vevo 770 imaging system (VisualSonics, Inc.) 24 hrs after surgery. The mice were anesthetized with 1.0–2.0% isoflurane and placed on a heating pad to maintain their body temperatures. The left ventricular dimensions were quantified by digitally recorded two-dimensional short-axis M-mode tracings at the level of the papillary muscles, to allow for consistent measurement at the same anatomic location in different mice; at least three consecutive beats were evaluated. Left ventricular (LV) wall thickness and internal dimensions were measured, and the LV ejection fraction (LVEF) was calculated.

Infarct size assessment. After 24 hrs of ischemia, the infarct size was determined with triphenyltetrazolium chloride (TTC) staining. Briefly, the mice were sacrificed, and the hearts were removed and sliced into five 1.0-mm thick sections perpendicular to the long axis. The sections were then incubated with 1% TTC (Sigma) in a phosphate solution at 37°C for 15 min. The areas of infarcted tissue (TTC-negative staining area) and the whole left ventricle were determined by computer morphometry using Bioquant imaging software.

H_2S levels in the cardiac tissue. The tissue concentration of H_2S was measured using a method described previously[35]. In brief, the mice were euthanized under anesthesia. The heart was flash-frozen with liquid nitrogen and then was homogenized in ice-cold potassium phosphate buffer. The homogenates were then centrifuged, and the supernatants were mixed with zinc acetate and water for 10 minutes at room temperature. Trichloroacetic acid was then added. The mixture was centrifuged, and the clear supernatant was collected and mixed with *N*, *N*-dimethyl-*p*-phenylenediamine sulfate and $FeCl_3$. After 20 minutes, the absorbance at 670 nm was measured by a microplate reader (Infinite 200; TECAN). The calibration curve of absorbance versus H_2S concentration was obtained using NaHS solutions at varying concentrations (0–320 μmol/L).

Flow cytometry analysis. A subset of six mice per group was used for flow cytometric analysis. The blood, spleen, and heart were collected and made into single-cell suspensions for flow cytometry, as previously described[11,34]. The cells were stained with a mixture of antibodies (anti-CD11b-FITC, anti-Gr-1-PerCP-Cy5.5; BD Biosciences). Data were acquired using an LSRII flow cytometer (BD Biosciences) and were analyzed with FlowJo7 software (Tree Star, Inc.).

Western blot. Proteins were extracted in a RIPA buffer from the whole mouse heart, and an equal number of proteins (30 μg) from each sample was separated by SDS-PAGE and was transferred onto a PVDF membrane (Merck Millipore). The membrane was blocked and incubated with primary antibodies (Bax, Bcl-2 from Cell Signaling Technology; caspase 3 from Bioworld) overnight at 4°C, followed by corresponding horseradish peroxidase-conjugated secondary antibodies (Jackson Laboratory). The blots were visualized with enhanced chemiluminescence and were quantified by densitometry.

Cardiomyocyte apoptosis. Cardiomyocyte apoptosis was evaluated via the terminal deoxynucleotidyl transferase-mediated dUTP nick-end labeling (TUNEL) method, using the ApopTag Peroxidase in Situ Apoptosis Detection Kit (Merck Millipore) according to the protocol provided by the manufacturer. The apoptosis index was determined by counting TUNEL-positive nuclei in five different fields per section, and it is expressed as a percentage of the total nuclei.

Measurement of cytokines. Blood was collected by cardiac puncture at the time of sacrifice. The samples were centrifuged, and the serum was collected according to the protocol provided by the manufacturer. The expressions of TNFα and IL-1β cytokines were measured with an ELISA Kit (R&D Systems).

Statistical analysis. The data are expressed as means ± SEMs. Different groups were compared by one-way ANOVA, followed by Tukey's or Bonferroni post-hoc test when applicable. Comparisons between the two groups were assessed by the *t* test. The Chi-square test (or Fisher's exact test when appropriate) was used to compare discrete variables between different groups. A P value less than 0.05 was considered significant.

1. Martelli, A. *et al.* Hydrogen sulphide: novel opportunity for drug discovery. *Med Res Rev* **32**, 1093–1130 (2012).
2. Shibuya, N. & Kimura, H. Production of hydrogen sulfide from d-cysteine and its therapeutic potential. *Front Endocrinol (Lausanne)* **4**, 87 (2013).
3. Wang, R. Two's company, three's a crowd: can H2S be the third endogenous gaseous transmitter? *FASEB J* **16**, 1792–1798 (2002).
4. Zhao, W., Zhang, J., Lu, Y. & Wang, R. The vasorelaxant effect of H(2)S as a novel endogenous gaseous K(ATP) channel opener. *EMBO J* **20**, 6008–6016 (2001).
5. Osipov, R. M. *et al.* Effect of hydrogen sulfide in a porcine model of myocardial ischemia-reperfusion: comparison of different administration regimens and characterization of the cellular mechanisms of protection. *J Cardiovasc Pharmacol* **54**, 287–297 (2009).
6. Xie, X. *et al.* Transplantation of mesenchymal stem cells preconditioned with hydrogen sulfide enhances repair of myocardial infarction in rats. *Tohoku J Exp Med* **226**, 29–36 (2012).
7. Dufton, N., Natividad, J., Verdu, E. F. & Wallace, J. L. Hydrogen sulfide and resolution of acute inflammation: A comparative study utilizing a novel fluorescent probe. *Sci Rep* **2**, 499 (2012).
8. Sivarajah, A. *et al.* Anti-apoptotic and anti-inflammatory effects of hydrogen sulfide in a rat model of regional myocardial I/R. *Shock* **31**, 267–274 (2009).
9. Swirski, F. K. *et al.* Identification of splenic reservoir monocytes and their deployment to inflammatory sites. *Science* **325**, 612–616 (2009).
10. Youn, J. I., Nagaraj, S., Collazo, M. & Gabrilovich, D. I. Subsets of myeloid-derived suppressor cells in tumor-bearing mice. *J Immunol* **181**, 5791–5802 (2008).
11. Yang, X. D. *et al.* Histamine deficiency promotes inflammation-associated carcinogenesis through reduced myeloid maturation and accumulation of $CD11b^+Ly6G^+$ immature myeloid cells. *Nat Med* **17**, 87–95 (2011).
12. Krum, H. & Teerlink, J. R. Medical therapy for chronic heart failure. *Lancet* **378**, 713–721 (2011).
13. Frangogiannis, N. G. Regulation of the inflammatory response in cardiac repair. *Circ Res* **110**, 159–173 (2012).
14. Naito, K. *et al.* Differential effects of GM-CSF and G-CSF on infiltration of dendritic cells during early left ventricular remodeling after myocardial infarction. *J Immunol* **181**, 5691–5701 (2008).
15. Anzai, A. *et al.* Regulatory role of dendritic cells in postinfarction healing and left ventricular remodeling. *Circulation* **125**, 1234–1245 (2012).
16. Yan, X. *et al.* Temporal dynamics of cardiac immune cell accumulation following acute myocardial infarction. *J Mol Cell Cardiol* **62**, 24–35 (2013).
17. Ganster, F. *et al.* Effects of hydrogen sulfide on hemodynamics, inflammatory response and oxidative stress during resuscitated hemorrhagic shock in rats. *Crit Care* **14**, R165 (2010).
18. Moody, B. F. & Calvert, J. W. Emergent role of gasotransmitters in ischemia-reperfusion injury. *Med Gas Res* **1**, 3 (2011).
19. Elrod, J. W. *et al.* Hydrogen sulfide attenuates myocardial ischemia-reperfusion injury by preservation of mitochondrial function. *Proc Natl Acad Sci U S A* **104**, 15560–15565 (2007).

20. Snijder, P. M. *et al.* Gaseous hydrogen sulfide protects against myocardial ischemia-reperfusion injury in mice partially independent from hypometabolism. *PLoS One* **8**, e63291 (2013).
21. Calvert, J. W. *et al.* Genetic and pharmacologic hydrogen sulfide therapy attenuates ischemia-induced heart failure in mice. *Circulation* **122**, 11–19 (2010).
22. Yang, G. *et al.* H2S as a physiologic vasorelaxant: hypertension in mice with deletion of cystathionine gamma-lyase. *Science* **322**, 587–590 (2008).
23. Yang, G. *et al.* Increased neointimal formation in cystathionine gamma-lyase deficient mice: role of hydrogen sulfide in alpha5beta1-integrin and matrix metalloproteinase-2 expression in smooth muscle cells. *J Mol Cell Cardiol* **52**, 677–688 (2012).
24. Gabrilovich, D. I. & Nagaraj, S. Myeloid-derived suppressor cells as regulators of the immune system. *Nat Rev Immunol* **9**, 162–174 (2009).
25. Srivastava, M. K., Sinha, P., Clements, V. K., Rodriguez, P. & Ostrand-Rosenberg, S. Myeloid-derived suppressor cells inhibit T-cell activation by depleting cystine and cysteine. *Cancer Res* **70**, 68–77 (2010).
26. Liao, Y. H. *et al.* Interleukin-17A contributes to myocardial ischemia/reperfusion injury by regulating cardiomyocyte apoptosis and neutrophil infiltration. *J Am Coll Cardiol* **59**, 420–429 (2012).
27. Liu, S. Q. *et al.* Endocrine Protection of Ischemic Myocardium by FGF21 from the Liver and Adipose Tissue. *Sci Rep* **3**, 2767 (2013).
28. Peake, B. F. *et al.* Hydrogen sulfide preconditions the db/db diabetic mouse heart against ischemia-reperfusion injury by activating Nrf2 signaling in an Erk-dependent manner. *Am J Physiol Heart Circ Physiol* **304**, H1215–1224 (2013).
29. Calvert, J. W. *et al.* Hydrogen sulfide mediates cardioprotection through Nrf2 signaling. *Circ Res* **105**, 365–374 (2009).
30. Piot, C. *et al.* Effect of cyclosporine on reperfusion injury in acute myocardial infarction. *N Engl J Med* **359**, 473–481 (2008).
31. Eltzschig, H. K. & Eckle, T. Ischemia and reperfusion--from mechanism to translation. *Nat Med* **17**, 1391–1401 (2011).
32. Zunnunov, Z. R. Efficacy and safety of hydrogen sulfide balneotherapy in ischemic heart disease the arid zone. *Ter Arkh* **76**, 15–18 (2004).
33. Kovacic, D. *et al.* Total plasma sulfide in congestive heart failure. *J Card Fail* **18**, 541–548 (2012).
34. Zhao, G. *et al.* CXCR6 deficiency ameliorated myocardial ischemia/reperfusion injury by inhibiting infiltration of monocytes and IFN-gamma-dependent autophagy. *Int J Cardiol* **168**, 853–862 (2013).
35. Qu, K., Chen, C. P., Halliwell, B., Moore, P. K. & Wong, P. T. Hydrogen sulfide is a mediator of cerebral ischemic damage. *Stroke* **37**, 889–893 (2006).

Acknowledgments

This study was supported by the State Key Development Program for Basic Research of China (No. 2011CB503905), the National Key Technology Support Program (No.2011BAI11B10), the Major Program of the National Natural Science Foundation of China (No.81230007), and the Shanghai Pujiang Program (12PJ1401700).

Author contributions

Y.E.Z. and H.L. conducted all statistical analyses and contributed to interpretation, writing sections of the manuscript. G.Z., Z.F.L. and H.M.Z. performed the experiment work. A.J.S., N.C.Z. and Y.Z.Z. conducted statistical analyses, designing figures. X.D.Y. contributed to the conceptualization and design of study, revising the earlier manuscript critically. J.B.G. contributed to design of study, revising the final manuscript critically. All authors discussed and commented on the manuscript.

Additional information

Competing financial interests: The authors declare no competing financial interests.

How to cite this article: Zhang, Y.E. *et al.* Hydrogen Sulfide Attenuates the Recruitment of $CD11b^{+}Gr\text{-}1^{+}$ Myeloid Cells and Regulates Bax/Bcl-2 Signaling in Myocardial Ischemia Injury. *Sci. Rep.* **4**, 4774; DOI:10.1038/srep04774 (2014).